

# System size resonance in an attractor neural network

M. A. DE LA CASA<sup>1</sup>(\*), E. KORUTCHEVA<sup>1</sup>(\*\*), J. M. R. PARRONDO<sup>2</sup> and F. J. DE LA RUBIA<sup>1</sup>

<sup>1</sup> *Dpto. Física Fundamental, Universidad Nacional de Educación a Distancia, c/Senda del Rey 9, 28040 Madrid, Spain*

<sup>2</sup> *Grupo Interdisciplinar de Sistemas Complejos (GISC) and Dep. Física Atómica, Molecular y Nuclear, Universidad Complutense, 28040 Madrid, Spain*

PACS. 05.70.Ln – Non-equilibrium and irreversible thermodynamics.

PACS. 05.40.Ca – Noise.

PACS. 07.05.+i – Neural networks.

**Abstract.** – We study the response of an attractor neural network, in the ferromagnetic phase, to an external, time-dependent stimulus, which drives the system periodically toward two different attractors. We demonstrate a non-trivial dependence of the response of the system via a system-size resonance, by showing a signal amplification maximum at a certain finite size.

*Introduction.* – The counter-intuitive role of fluctuations as a source of order has attracted much attention for the last years [1, 2]. Particularly interesting is the phenomenon of stochastic resonance where the response of a non-linear system to the action of a weak signal is enhanced, not hindered, by the addition of an optimal amount of noise [3]. Among several potential applications of stochastic resonance, there is evidence that it plays an important role in some cognitive processes, such as perception [4–6].

Another phenomenon that recently appeared in the literature and is closely related to stochastic resonance is system size resonance, or SSR from now on [7]. In SSR, the presence of noise in a system of finite size, close to a second-order phase transition, gives rise to the appearance of an optimal size for the system to adapt to an external field [7–9].

Inspired by the applications of stochastic resonance to cognitive processes, in this Letter we show that SSR can operate in a simple model of associative memory, namely, a Hopfield neural network [10], improving its ability to follow a time-dependent stimulus. We will focus on the simplest case of a Hopfield network storing just two patterns.

*Model.* – The model is defined by the following Hamiltonian [10]:

$$\mathcal{H} = -\frac{1}{N} \sum_{i < j} J_{ij} s_i s_j - h \sum_i \xi_i^{\mu(t)} s_i, \quad (1)$$

---

(\*) E-mail: [macasa@fisfun.uned.es](mailto:macasa@fisfun.uned.es)

(\*\*) also G.Nadjakov Inst.Solid State Physics, Bulgarian Academy of Sciences, 1784 Sofia, Bulgaria

where  $s_i = \pm 1, i = 1, \dots, N$  are  $N$ -binary neurons and  $\xi_i^\mu = \pm 1, i = 1, \dots, N, \mu = 1, 2$  are the two binary patterns the system is trained with. We assume that the network has been trained following the Hebb rule [11]:

$$J_{ij} = \xi_i^1 \xi_j^1 + \xi_i^2 \xi_j^2. \quad (2)$$

The second term in Eq. (1) represents a non constant but periodic stimulus of period  $2T$ :  $\mu(t) = 1$  if  $t \in [0, T)$  and  $\mu(t) = 2$  if  $t \in [T, 2T)$ , which biases the system towards pattern 1 and 2, alternatively. The intensity of the stimulus is given by  $h$ .

A relevant magnitude in our analysis is the Hamming distance between the patterns:

$$d = \frac{1}{2N} \sum_{i=1}^N |\xi_i^1 - \xi_i^2|, \quad (3)$$

i.e., the fraction of sites in which both patterns are different. It varies between 0, when both patterns are equal at every site, and 1 when they are completely different.

This system has been extensively studied in the literature, mainly in the thermodynamic limit  $N \rightarrow \infty$  (see [12, 13] and the references therein). The role of finite size has only been studied in order to find finite-size corrections to infinite-size results [14]. In this work, we keep  $N$  explicitly finite and focus on the effect of the finite size on the response of the system to the time-dependent stimulus.

*Equilibrium states.* – The two following order parameters are usually defined to describe the macrostate of the network:

$$m_\mu = \frac{1}{N} \sum_i \xi_i^\mu s_i, \quad (4)$$

which are the overlaps between each pattern and the neurons.

However, these two parameters are not independent. A more convenient pair of magnitudes can be defined as follows:  $r$  is the fraction of bits where  $\{s_i\}$  coincides both with pattern 1 and 2;  $p$  is the fraction of bits where  $\{s_i\}$  coincides with pattern 1 and differs from pattern 2. In Fig. 1 we have plotted a schematic representation of the two patterns and the quantities  $p$  and  $r$ . Taking into account that  $m_\mu$  is the fraction of common bits minus the fraction of different bits between the network and pattern  $\xi^\mu$ , from Fig. 1 one immediately obtains:

$$m_1 = 2r + 2p - 1; \quad m_2 = 2r + 2d - 2p - 1. \quad (5)$$

Also from this figure, it is easy to see that  $r$  and  $p$  are independent and can take on any value in the rectangle:  $r \in [0, 1-d]$ ,  $p \in [0, d]$ . Moreover, in terms of  $r$  and  $p$ , the free energy of the system for  $h = 0$  can be written as

$$\mathcal{F} = \mathcal{F}_r + \mathcal{F}_p \quad (6)$$

with

$$\begin{aligned} \mathcal{F}_r &= -4N \left( r - \frac{1-d}{2} \right)^2 - \frac{1}{\beta} \log \left( \frac{N(1-d)}{Nr} \right) \\ \mathcal{F}_p &= -4N \left( p - \frac{d}{2} \right)^2 - \frac{1}{\beta} \log \left( \frac{Nd}{Np} \right). \end{aligned} \quad (7)$$

At zero temperature, the free energy has four minima, located at the corners of the available rectangle in the parameter space, i.e.,  $r = 0, 1-d$ , and  $p = 0, d$ . Two of the four equilibrium

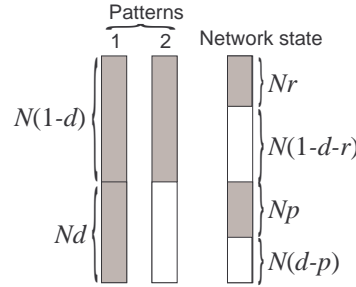


Fig. 1 – Schematic representation of the two patterns and the state of the network. The upper part of the patterns represents the  $N(1 - d)$  coincident bits between the patterns.  $Nr$  is the number of bits that the network has in common with both patterns, whereas  $p$  is number of bits in the network coinciding with pattern 1 and different from pattern 2.

states,  $r = 1 - d$ ,  $p = 0, d$ , exactly reproduce the two patterns. The other two minima,  $r = 0$ ,  $p = 0, d$ , are the negatives of the stored patterns. Fig. 2 a) shows a typical landscape of the free energy in the  $(r, p)$  plane for low temperatures ( $\beta = 2$ ,  $d = 0.7$ ).

If we increase the temperature, the four minima shift to the middle point of the rectangle  $r = (1 - d)/2$  and  $p = d/2$ . In the thermodynamic limit, the system undergoes two second-order phase transitions at  $\beta_{c,r} = 1/(2 - 2d)$  and  $\beta_{c,p} = 1/(2d)$ . In each transition the minima collide into either  $r = (1 - d)/2$  or  $p = d/2$ , which corresponds, respectively, to a completely disordered state in the region of common and distinct bits between the two patterns (see Fig. 1). The ability of the network to distinguish between the two patterns sensibly depends on which of the two transitions occurs first.

If  $d < 0.5$ , i.e., if the two patterns share more than a half of the bits,  $\beta_{c,p} > \beta_{c,r}$ . Consequently, when the temperature increases from absolute zero the first transition occurs for the variable  $p$ , i.e., in the region of distinct bits. This means that for temperatures  $\beta \in [\beta_{c,r}, \beta_{c,p}]$ , the system only exhibits two minima with  $p = d/2$ , i.e., with  $m_1 = m_2$  [see Eq. (5)]. One of these two minima approximately reproduces the common bits of the two patterns, whereas the distinct bits are completely disordered. The other minima is just the negative image of the first. Consequently, the system has mixed up the two patterns and it is unable to distinguish between them. The free energy landscape corresponding to this situation is plotted in Fig. 2 b).

On the other hand, if  $d > 0.5$ , the two patterns are different enough to be distinguished even for intermediate temperatures. In this case  $\beta_{c,r} > \beta_{c,p}$ , and the first transition occurs at  $\beta_{c,r}$ . Therefore, if  $\beta \in [\beta_{c,p}, \beta_{c,r}]$ , we have two minima with  $r = (1 - d)/2$ , i.e., with  $m_1 = -m_2$ . One of the two minima reproduces the distinct bits of pattern 1 and the other one the distinct bits of pattern 2. For both minima, the common bits are disordered. Although the system does not exactly reproduce the stored patterns, it perfectly distinguishes between them. The free energy in this case is plotted in Fig. 2 c).

Finally, above the maximum critical temperature, the only equilibrium state is completely disordered:  $r = (1 - d)/2$  and  $p = d/2$ , or  $m_1 = m_2 = 0$ , as shown in Fig. 2 d).

Along this Letter we will focus only on the third case: patterns with  $d > 0.5$  and temperatures corresponding to the landscape in Fig. 2 c). The reason is that the system still distinguishes between the two patterns, but we can reach temperatures high enough to clearly observe SSR.

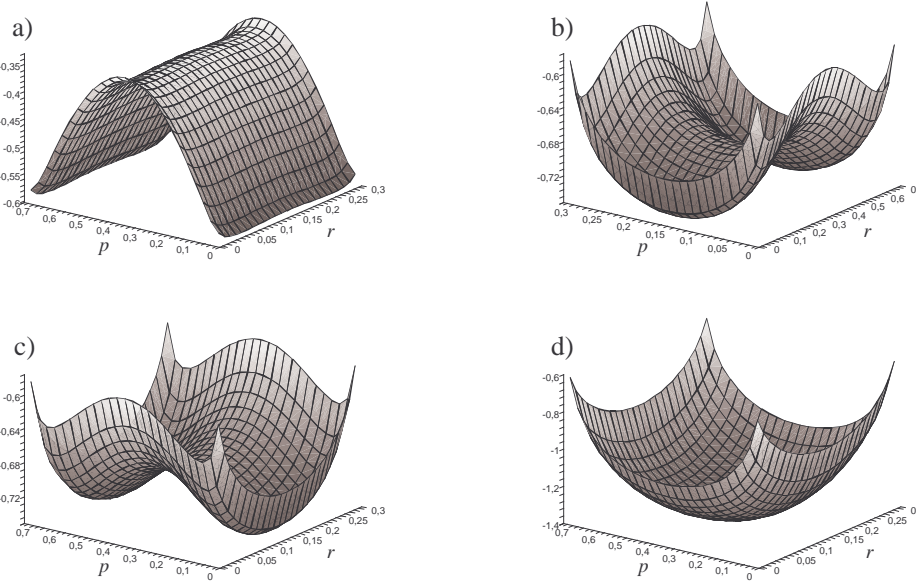


Fig. 2 – The free energy landscape for  $h = 0$  and  $N = 10000$ . a) *Low temperature,  $\beta = 2, d = 0.7$ :* The free energy presents four minima, corresponding to the two stored patterns and their respective negatives. b) *Medium temperature, similar patterns,  $\beta = 1, d = 0.3$ :* There are two equilibrium states with  $p = d/2$ , i.e., with  $m_1 = m_2$ . One of the minima reproduces the common bits of the two patterns whereas the other one is its negative. c) *Medium temperature, dissimilar patterns,  $\beta = 1, d = 0.7$ :* There are two equilibrium states with  $r = (1 - d)/2$ , i.e., with  $m_1 = -m_2$ . Each minima reproduces the distinct bits of each pattern. d) *High temperature,  $\beta = 0.5, d = 0.7$ :* The only minimum is the disordered state with  $r = (1 - d)/2$ ,  $p = d/2$ , i.e., with  $m_1 = m_2 = 0$ .

*Results.* – We have performed out-of-equilibrium Monte Carlo simulations [15] at inverse temperature  $\beta$  using the Hamiltonian (1). The dynamics is defined by a standard Metropolis algorithm in which 100000 sweeps have been carried out averaging over 100 realizations for every parameter set.

The simulations show a clear evidence of SSR. A relevant example is presented in Fig. 3, with the distinctive features of stochastic resonance. For small  $N$ , fluctuations are strong and the system output is too noisy being unable to retrieve the patterns dynamically. The hoping between the attractors is random and not synchronized with the switches of the external stimulus. For very large  $N$ , fluctuations are weak and the system is quenched in a given attractor. However, for intermediate values of  $N$ , the system follows the oscillations of the external stimulus and the appropriate pattern for every half-period is retrieved very precisely. In order to obtain a more quantitative picture of SSR, we use the power spectrum  $S_m(\omega)$  of one of the order parameters. We will focus on the power spectrum of  $m_1(t)$ , but similar results are obtained if  $m_2(t)$  is chosen. A measure of the quality of the response of the system to the external input is the so-called *signal amplification*  $\eta$  [16], defined as the ratio between the power spectrum at the external frequency  $\Omega = \pi/T$  and the total power contained in the external stimulus:

$$\eta = \lim_{\Delta\omega \rightarrow 0} \frac{2 \int_{\Omega - \Delta\omega}^{\Omega + \Delta\omega} S_m(\omega) d\omega}{h^2}. \quad (8)$$

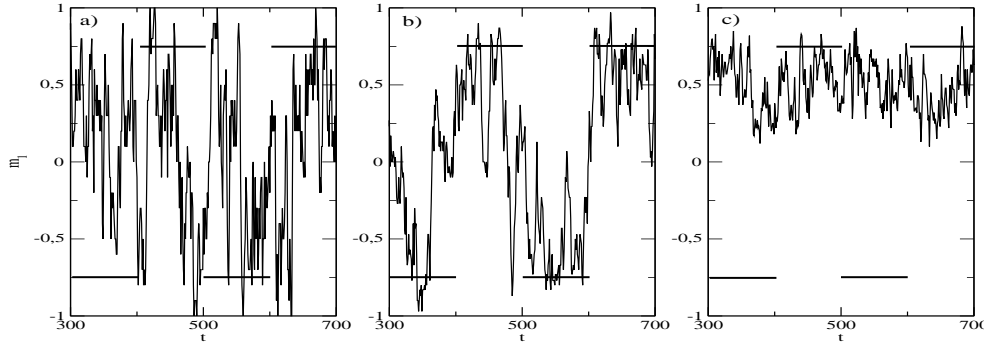


Fig. 3 – Time evolution of the order parameter  $m_1$  showing the first evidence of system-size resonance. The solid thin line is the order parameter obtained from numerical simulations. The thick segments show the time intervals in which the external stimulus drives the system to retrieve one or the other pattern. The parameters values are:  $\beta = 1.2$ ,  $d = 0.6$ ,  $T = 100$ ,  $h = 0.01$ . a)  $N = 20$ ; b)  $N = 60$ ; c)  $N = 120$ .

Following previous work [7, 16], we will use the signal amplification  $\eta$  to locate and assess resonance phenomena.

We have also obtained an analytical expression for  $S_m(\omega)$  reproducing quite well the numerical experiments. The main idea is to approximate the dynamics of the network by a two-state system and follow the calculation performed in [3, 17]. The details of the theory will be presented in a forthcoming publication [18]. Here we will only sketch the main steps of the calculation.

The starting point is a master equation for the two-state system. The states are the two minima of the free energy, which are located numerically. As shown above, each of these minima reproduces fairly well the two stored patterns, hence we label them as 1 and 2. The transition probabilities between these two states  $W_{1 \rightarrow 2}$  and  $W_{2 \rightarrow 1}$  depend on time as  $W_{1 \rightarrow 2}(\mu(t))$ ,  $\mu(t)$  being the pattern shown to the network at time  $t$ . We have chosen an Arrhenius-like expression as in [3, 17]:

$$\begin{aligned} W_{1 \rightarrow 2}(1) &= c \exp(-\beta \Delta \mathcal{F}) \exp(-\beta h d_{12} N / 2) \\ W_{1 \rightarrow 2}(2) &= c \exp(-\beta \Delta \mathcal{F}) \exp(\beta h d_{12} N / 2), \end{aligned} \quad (9)$$

where  $d_{12}$  is the difference between the values of the order parameter  $m_1$  in the two minima,  $\Delta \mathcal{F}$  is the free energy barrier separating, at zero external field, the two minima along the path  $r = (1 - d)/2$ , with  $m_1 = -m_2$ , and  $c$  is an arbitrary constant (see panel c in Fig. 2). The transition probabilities  $W_{i \rightarrow j}$  are chosen to satisfy detailed balance:  $W_{1 \rightarrow 2}(1) = W_{2 \rightarrow 1}(2)$ .

The corresponding master equation for this two-state stochastic process can be solved exactly to get the time-dependent moments  $\langle m_1(t) \rangle$  and  $\langle m_1(t)m_1(t + \tau) \rangle$ . Finally, by using Wiener-Khinchin theorem [19], we obtain the following explicit expression for the power spectra  $S_m(\omega)$ :

$$\begin{aligned} S_m(\omega) &= \frac{d_{12}^2}{4} \left[ 1 - \tanh^2(\beta h d_{12} N) \left( 1 - \frac{2\Omega}{\pi W} \tanh\left(\frac{\pi W}{2\Omega}\right) \right) \right] \frac{2W}{\omega^2 + W^2} \\ &+ \frac{2d_{12}^2}{\pi} \tanh^2(\beta h d_{12} N) \sum_{k=1}^{\infty} \frac{W^2}{(2k-1)^2(W^2 + (2k-1)^2\Omega^2)} \\ &\times (\delta[\omega - (2k-1)\Omega] + \delta[\omega + (2k+1)\Omega]) \end{aligned} \quad (10)$$

with

$$W = W_{1 \rightarrow 2}(1) + W_{1 \rightarrow 2}(2) = c \exp(-\beta \Delta \mathcal{F}) \cosh(\beta h d N). \quad (11)$$

The resonant behavior of the signal amplification  $\eta$  can be seen in Fig. 4. There is a maximum

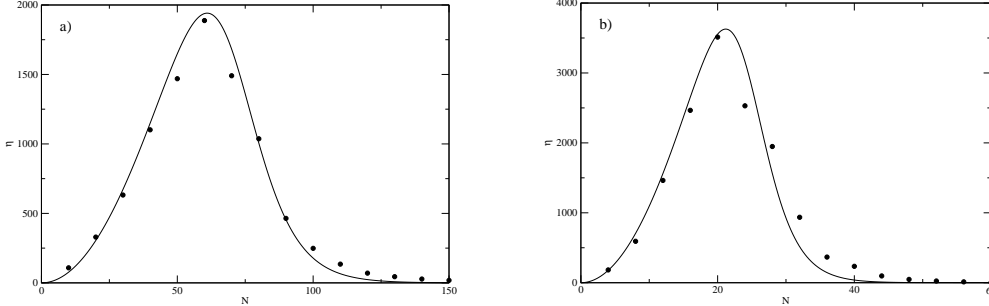


Fig. 4 – The signal amplification,  $\eta$ , versus the size of the system,  $N$  for  $h = 0.01$ . The result of the numerical simulation is represented by dots while the analytical result is the solid line. a)  $d = 0.6$ ,  $T = 500$ ,  $\beta = 1.2$ . b)  $d = 0.75$ ,  $T = 500$ ,  $\beta = 1.2$ . For larger values of  $d$ , the maximum is shifted to the left. The only free parameter in this theory is  $c$ , which has been chosen to fit best the Monte Carlo data. In a),  $c = 0.44$ ; in b),  $c = 0.65$ .

of the signal amplification at a finite size. The results of the numerical simulation (dots) correspond very well to the analytical results (solid line) given by Eq. (10). The difference between both panels of Fig. 4 is exclusively due to a difference in the value of the Hamming distance  $d$ , keeping the other parameters  $\Omega$ ,  $h$  and  $\beta$  equal. A larger value of  $d$  implies a higher energy barrier between the attractors which needs a larger noise intensity or smaller  $N$  to achieve the best resonance. Consequently, the maximum of  $\eta$  is shifted towards smaller  $N$ , and its maximum resonant value is reduced. Finally the dependence of  $\eta$  on the stimulus

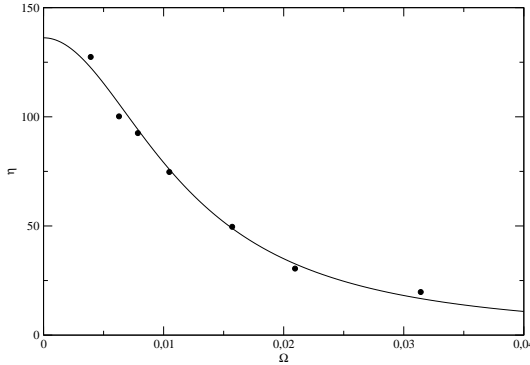


Fig. 5 – The behavior of  $\eta$  as a function of the frequency  $\Omega$  of the external stimulus shows the expected Lorentzian form, as in usual stochastic resonance. Again, the dots represent the numerical simulations and the solid line the analytical results. In this plot,  $d = 0.6$ ,  $N = 50$ ,  $\beta = 1.2$  and  $h = 0.01$ .  $c=0.44$ , as in panel a) in Fig. 4.

frequency  $\Omega$  is shown in Fig. 5. It shows the Lorentzian dependence expected in SR [3,20]. A good agreement between theory and numerical simulations is observed as well.

*Conclusions.* – In this paper we have presented numerical simulations and theoretical calculations, based on a two-state model, showing the presence of system size resonance effects in an attractor neural network. These effects are made evident by the resonant behavior of the signal amplification  $\eta$  as a function of the size of the system, as well as by the time evolution of the order parameters. We also point out the good agreement between analytical results and simulations.

Our model shows that noise can provide the flexibility that an adaptive memory needs to follow a time-dependent stimulus. Since noise depends on the size of the system, we conclude that there is an optimal size for which there is maximal synchronization of the system to the evolving stimulus. We have explicitly shown this resonant phenomenon in a simple model with two attractors, but it is likely that more complicated models exhibit the same effect.

\*\*\*

This work is financially supported by Ministerio de Ciencia y Tecnología (Spain), Projects No. BFM2001-291 and FIS2004-271, and by UNED, Plan de Promoción de la Investigación 2002.

## REFERENCES

- [1] HORSTHEMKE W. and LEFEVER R., *Noise-induced transitions* (Springer-Verlag, Berlin) 1984.
- [2] GARCÍA-OJALVO J. and SANCHO J. M., *Noise in spatially extended systems* (Springer-Verlag, New York) 1999.
- [3] GAMMAITONI L., HÄNGGI P., JUNG P. and MARCHESONI F., *Rev. Mod. Phys.*, **70** (1998) 223.
- [4] RIANI M., SEIFE C., ROBERTS M., TWITTY J., and MOSS F., *Phys. Rev. Lett.*, **78** (1997) 1186.
- [5] RUSSELL D.F., WILKENS L.A., and MOSS F., *Nature*, **402** (1999) 291.
- [6] HIDAKA I., NOZAKI D., and YAMAMOTO Y., *Phys. Rev. Lett.*, **85** (2000) 3740.
- [7] PIKOVSKY A., ZAIKIN A. A. and DE LA CASA M. A., *Phys. Rev. Lett.*, **88** (2002) 050601.
- [8] TORAL R., MIRASSO C. R. and GUNTON J. D., *Europhys. Lett.*, **61** (2003) 162.
- [9] SCHMID G., GOYCHUK I., HANGGI P., ZENG S. and JUNG P., *Fluctuations and Noise Letters*, **4** (2004) L33.
- [10] HOPFIELD J., *Proc. Natl. Acad. Sci. USA*, **79** (1982) 2554.
- [11] HEBB D., *The organization of behavior: a neurophysiological theory* (Wiley, New York) 1949.
- [12] SPECIAL ISSUE IN MEMORY OF ELIZABETH GARDNER, *J. Phys. A: Math. Gen.*, **22** (1989) 1959-2265.
- [13] HERTZ J., KROGH A. and PALMER R., *Introduction to the theory of neural computation* (Addison-Wesley, New York) 1991.
- [14] PRIVMAN V., *Finite-size scaling and numerical simulations of statistical systems* (World Scientific, Singapore) 1990.
- [15] NEWMAN M. E. J. and BARKEMA G. T., *Monte Carlo methods in statistical physics* (Clarendon Press, Oxford) 1999, sect. II.
- [16] JUNG P., and HÄNGGI P., *Phys. Rev. A*, **44** (1991) 8032.
- [17] McNAMARA B. and WIESENFELD K., *Phys. Rev. A*, **39** (1989) 4854.
- [18] DE LA CASA M. A., KORUTCHEVA E., J.M.R. PARRONDO and DE LA RUBIA, F. J., *in preparation*.
- [19] GARDINER C. W., *Handbook of stochastic methods* (Springer-Verlag, Berlin) 1983.
- [20] JUNG P., *Phys. Reports*, **234** (1993) 175.